J. Korean Powder Metall. Inst., Vol. 23, No. 2, 120-125, 2016
DOI: 10.4150/KPMI.2016.23.2.120

Investigation of Ball Size Effect on Microstructure and Thermoelectric Properties of *p*-type BiSbTe by Mechanical Alloying

May Likha Lwin, Sang-min Yoon, Babu Madavali, Chul-Hee Lee, and Soon-Jik Hong*
Division of Advanced Materials Engineering, Kongju National University, 275, Budae-Dong, Cheonan City, Chungcheongnam-do 32588, Korea
(Received March 28, 2016; Revised April 18, 2016; Accepted April 20, 2016)

Abstract *P*-type ternary $Bi_{0.5}Sb_{1.5}Te_3$ alloys are fabricated via mechanical alloying (MA) and spark plasma sintering (SPS). Different ball sizes are used in the MA process, and their effect on the microstructure; hardness, and thermoelectric properties of the *p*-type BiSbTe alloys are investigated. The phases of milled powders and bulks are identified using an X-ray diffraction technique. The morphology of milled powders and fracture surface of compacted samples are examined using scanning electron microscopy. The morphology, phase, and grain structures of the samples are not altered by the use of different ball sizes in the MA process. Measurements of the thermoelectric (TE) transport properties including the electrical conductivity, Seebeck coefficient, and power factor are measured at temperatures of 300-400 K for samples treated by SPS. The TE properties do not depend on the ball size used in the MA process.

Keywords: $Bi_{0.5}Sb_{1.5}Te_3$ alloys, Mechanical alloying, Spark plasma sintering, Thermoelectric properties

1. Introduction

Thermoelectric materials are solid-state devices that are used for refrigeration and power generation based on the thermoelectric effects. The performance of the thermoelectric materials is defined by the dimensionless figure of merit, *ZT*:

$$ZT = (\alpha^2\sigma/\kappa)\, T \quad (1)$$

Where α, σ, κ and T are the Seebeck coefficient, electrical conductivity, thermal conductivity and the absolute temperature [1-3]. High-efficiency thermoelectric materials should have large Seebeck coefficient, high electrical conductivity, and low thermal conductivity. However, there is no existence of such ascribed characteristics of the material in nature, so it is a central issue in thermoelectric research to increase *ZT* with balancing all TE properties each other [4].

Bismuth antimony telluride (BiSbTe) alloys have been used in thermoelectric modules that show excellent TE properties at ambient room temperature [5, 6], and much work has been done to enhance their *ZT* values. Rama et al. reports a *ZT* >2.4 by creation of quantum dot superlattice of BiSbTe with low lattice thermal conductivity [7]. Though these materials exhibited the improved TE properties, it is highly impossible for large-scale energy conversion applications due to limitations in both heat transfer and cost. Later, Ren and Chen *et al.* fabricated nanostructured BiSbTe bulks and reported a peak *ZT* of 1.4 at 100ºC by mechanical alloying and hot pressing. Also, hot extrusion [8], and spark plasma sintering [9] are used to fabricate BiSbTe based alloys with improved performance. The substantial improvement of *ZT* in BiSbTe is attributed to the dramatic reduction in thermal conductivity caused by severe phonon scattering by the numerous interfaces in nanostructured bulk samples [10, 11]. Mechanical alloying (MA) is an eminent process to fabricate nanopowder from the commercial ingots or elemental chunks. MA allows the formation of extremely fine solid solutions of required alloys from the starting materials through a sequence of collision events inside ball mill [12]. In another hand, SPS is a low temperature sintering technique in which the grain growth can be prevented due to short sintering time than the conventional meth-

*Corresponding Author: Soon-Jik Hong, **TEL:** +82-41-521-9387, **FAX:** +82-41-568-5776, **E-mail:** hongsj@kongju.ac.kr

ods [9]. Li *et al.* compared TE properties in AgPbSbTe alloys made by vacuum melting and MA+SPS process and revealed that MA with SPS shows excellent TE properties [13]. It is known that the ball milling parameters can influence the microstructure and TE properties 14]. Sandra *et al* studied TE properties of BiSbTe based alloys by varying milling times in MA and reported 5h milling exhibit *ZT* of 1.3 due to its low lattice thermal conductivity [12]. Nevertheless, the effect of ball sizes in MA of BiSbTe has not been reported.

In this research, *p*-type BiSbTe fine powders are fabricated by MA from commercially available micron size powders. Subsequently, the milled powders are sintered by SPS at 400ºC for 10 min. The effect of ball sizes (during the milling process) on microstructures, mechanical and thermoelectric properties are investigated.

2. Experimental Procedure

Commercial $Bi_{0.5}Sb_{1.5}Te_3$ powders (size < 200 μm) were used for fabrication of fine powders using different ball sizes (3 mm, 5 mm and 10 mm). The process was carried out in a planetary ball miller in argon atmosphere. The ball to powder ratio were kept at 15:1 with 1100 revolutions per minute (rpm). Subsequently, the milled powders were sintered by SPS under an axial compressive stress of 50 MPa at 673K for 10 min in vacuum. The sintered bulks are disc with dimensions of approximately 20 mm in diameter and 6 mm in thickness.

The phase of the pellets was analyzed with an XRD (X- ray diffraction) Rigaku Miniflex diffractometer using CuK_α radiation. The morphology of the mechanically milled powders and fracture surface of SPS-ed bulks were analyzed by scanning electron microscopy (SEM-MIRA LMH II (TESKAN), Czech Republic). The oxygen content of the powders was determined by the of Eltra ONH-2000 Oxygen/Nitrogen/Hydrogen determinator. The relative densities of the samples were measured from the Archimedes principle. The micro Vickers hardness tester was used to measure the hardness of the samples.

The samples were cut into rectangular pieces (3 × 3 × 10 mm^3) for Seebeck coefficient and electrical conductivity and measured by the thermoelectric power (TEP-1000) measurement system. The carrier concentration and hall mobility were measured from the four-probe method

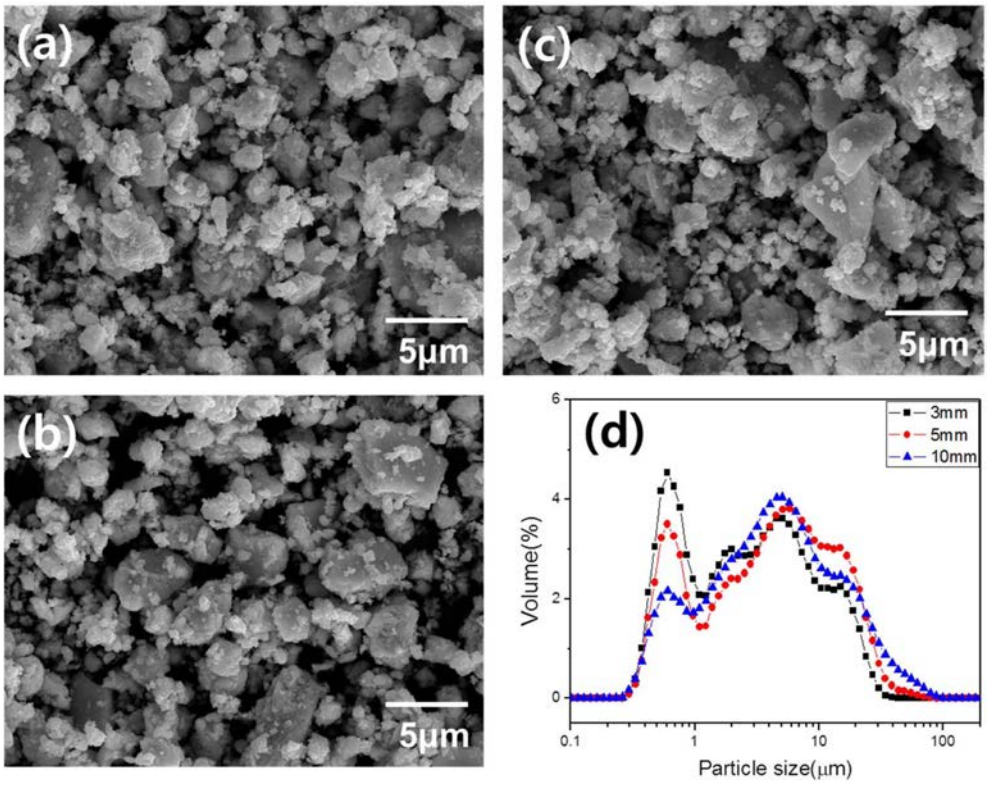

Fig. 1. Morphology of p-type BiSbTe powders using different ball sizes during MA (a) 3 mm, (b) 5 mm, (c) 10 mm, and (d) powder size analysis of MA-ed powders.

at room temperature. The power factor was calculated from the multiply of the square of the Seebeck coefficient and electrical conductivity.

3. Results and Discussion

The morphology of the *p*-type BiSbTe powders using different ball sizes during the MA process are presented in Fig. 1. All the powders (Fig. 1(a)-(c)) exhibited the same morphology albeit with slight differences. It can be observed from the morphologies that the powders particle is irregular in shapes with a distribution of very fine particles to large particles. Some particle agglomerated with each other regardless of different ball sizes used in the milling process [14]. The particle size analysis is presented in the Fig. 1(d). It is clearly seen that the distribution is expanded from submicron order to ~40 μm range. The high order particle sizes from the agglomeration of the fine particles during the milling process. It is necessary to analyze the oxygen contamination in milled powders, which can affect the microstructures, mechanical properties, and TE properties as well [15]. The oxygen impurity in milled powders is shown in Table 1. The oxygen impurity is measured about ~0.37 wt% for all powders regardless of processing parameters, which is very low in amount and can be expected to be minimized after sintering. The mechanically milled powders (by different ball sizes 3, 5, and 10 mm during MA) are subsequently sintered by spark plasma sintering (SPS). The relative densities are measured over 99.8% of all SPS-ed bulks, which are listed in Table 1. The micro Vickers hardness of the bulks are measured as 97, 102, and 105 Hv for 3, 5 and 10 mm balls sizes used in the milling process respectively, however one can conclude that there is no strong influence of the ball size on hardness during the MA process.

Table 1. Oxygen content, relative density and micro Vickers hardness of p-type BiSbTe alloys by mechanical milling

Ball Size	Oxygen Content (%)	Relative density (%)	Micro-Vickers Hardness (Hv)
3 mm	0.378	99.9	97
5 mm	0.37	99.9	102
10 mm	0.313	99.8	105

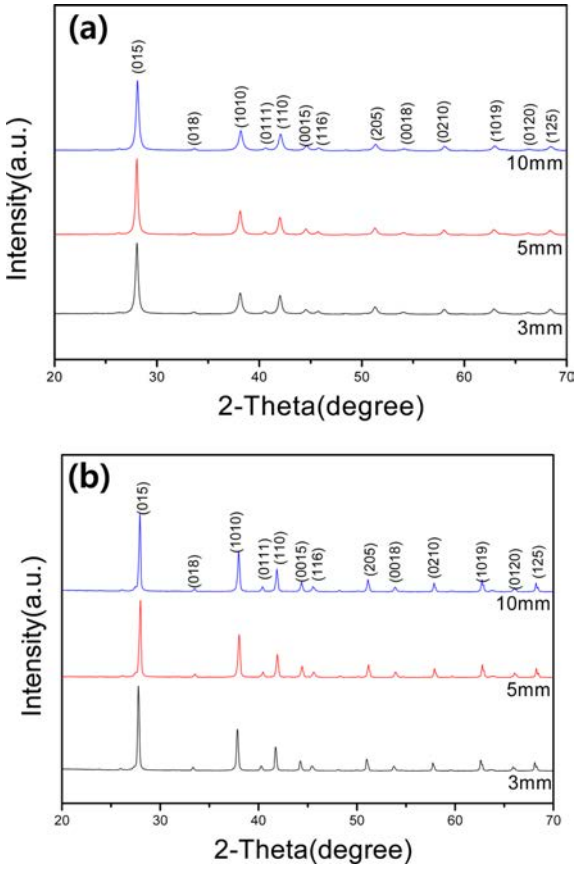

Fig. 2. XRD analysis of (a) MA-ed powders and (b) SPS-ed bulks of p-type BiSbTe alloys.

Fig. 2 shows the XRD pattern of *p*-type BiSbTe milled powders and SPS-ed bulks using different ball sizes in MA process. As shown in Fig. 2, all powders and bulk samples maintain the single phase of $Bi_{0.5}Sb_{1.5}Te_3$ with JCPDS # 49-1713. It is clearly seen in the XRD pattern that the both basal planes and non-basal planes exhibited same peak intensity without any shifting in position. It revealed that there is no lattice deformation and orientation in the *p*-type BiSbTe bulks. No other impurities are detected in the XRD analysis.

Fig. 3 shows the SEM fracture surfaces of *p*-type BiSbTe bulks usage different ball sizes during the milling process. The grains are distributed uniformly throughout the matrix with smooth and laminar surfaces. The grain sizes are distributed from submicron order to ~4 μm, which growth strictly retarded during the low temperature SPS process. All the bulk samples exhibited almost uniform grain distribution regardless of their MA parameters (ball size variation).

Temperature dependence of thermoelectric Seebeck coeffi-

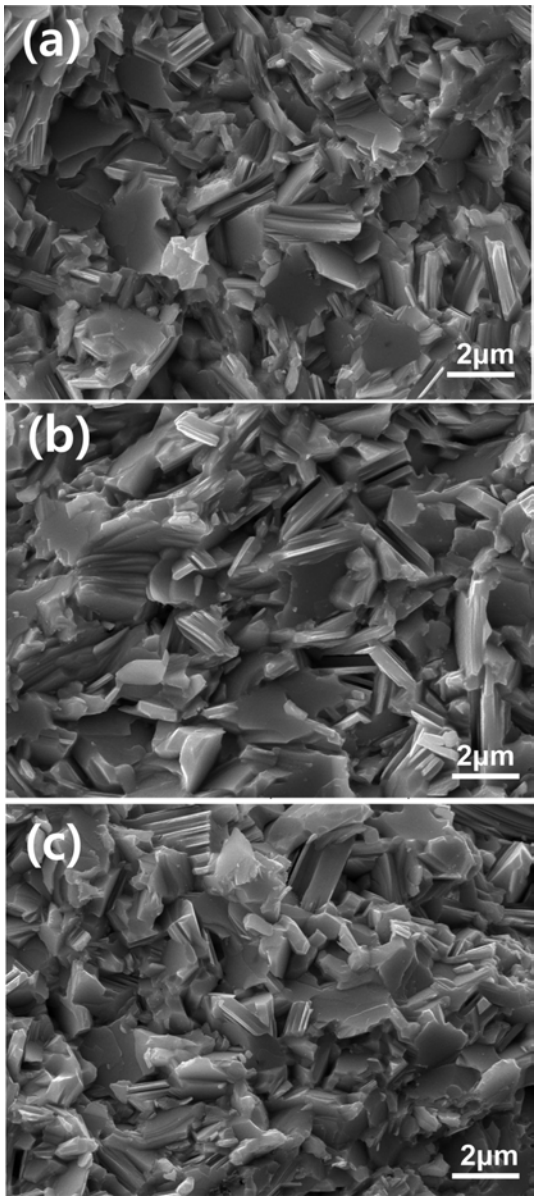

Fig. 3. Fracture surface analysis of p-type BiSbTe bulks using different ball sizes during MA (a) 3 mm, (b) 5 mm, and (c) 10 mm.

cient α for *p*-type BiSbTe bulks with different processing parameters is shown in Fig. 4. It is evident from Fig. 4 that the Seebeck coefficient is positive over the temperature range indicating a *p*-type semiconducting behavior [12]. The Seebeck coefficient is increased with increasing measurement temperature, which was consistent with earlier reported studies [12]. The Seebeck coefficient shows almost same values regardless of ball sizes used during the MA process. In general, the Seebeck coefficient is expressed as follows [16]:

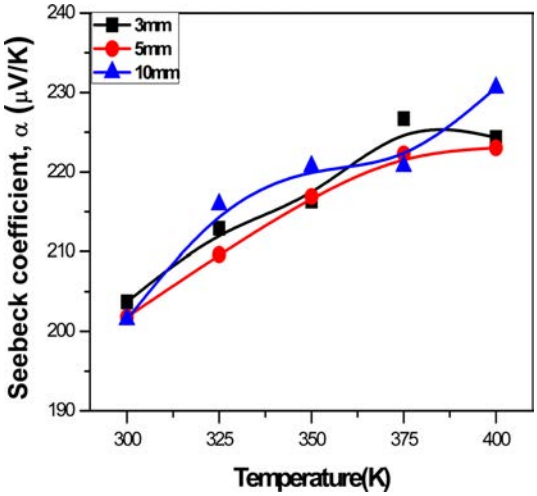

Fig. 4. Temperature dependence of Seebeck coefficient for p-type BiSbTe bulks using different ball sizes during MA.

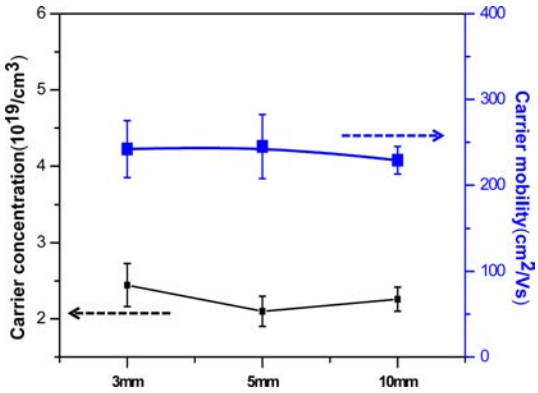

Fig. 5. Carrier concentration and mobility for p-type BiSbTe bulks using different ball sizes during MA.

$$\alpha = \gamma - ln\, n_c \tag{2}$$

where γ is scattering parameter, n_c is the carrier concentration. It is known that the carrier concentration greatly contributes to the Seebeck coefficient [12]. The carrier concentration and carrier mobility are shown in Fig. 5. It is observed that the carrier concentration of *p*-type BiSbTe specimens are almost uniform in values and of the order of 10^{19} per cubic meter. The γ term results from the scattering of carriers at numerous grain boundaries [11]. It can be clearly seen from the Fig. 5 that the carrier mobility is almost same for all samples. Therefore, it is expected that the scattering of carriers at the grain boundaries are same in all the bulk samples which resulted in the obtained Seebeck coefficient been of the same order for all samples regardless of processing parameters.

The temperature dependence of electrical conductivity,

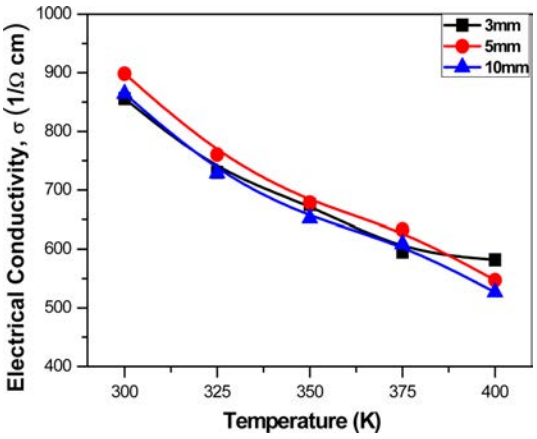

Fig. 6. Temperature dependence of electrical conductivity for p-type BiSbTe bulks using different ball sizes during MA.

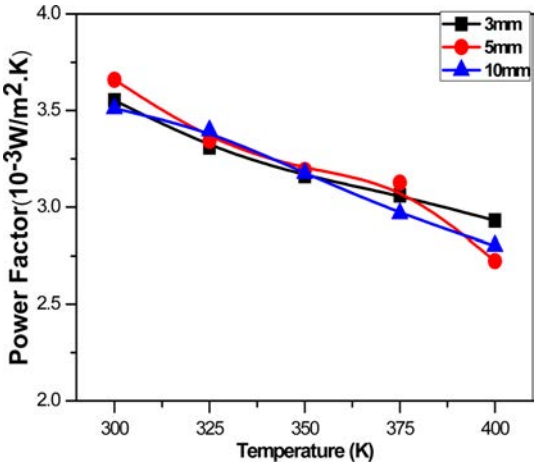

Fig. 7. Temperature dependence of power factor for p-type BiSbTe bulks using different ball sizes during MA.

σ for *p*-type BiSbTe bulks with different processing parameters are shown in Fig. 6. The electrical conductivity decreases with increasing temperature, which indicates that all samples exhibited metal-like behavior or degenerate semiconductor behavior [14]. The measured electrical conductivity is almost same for all samples regardless of processing parameters. Nevertheless, σ shows maximum value about 898 1/Ω cm at room temperature and decreased ~550 1/Ω cm. In general, σ is given by [16],

$$\sigma = n_c e \mu \quad (3)$$

where e is the carrier charge. It is evident from the Fig. 5 that both n_c, μ are un-altered with processing parameters resulting in almost no variation in electrical conductivity for all samples.

Fig. 7 shows the temperature dependence of power factor for *p*-type BiSbTe bulks with different processing parameters. The power factor values are calculated from the multiple of the square of the Seebeck coefficient and electrical conductivity. It is observed that the calculated power factor values decrease with increasing temperature, which is quite similar with their Seebeck coefficient and electrical conductivity results. The calculated power factor is almost of the same order regardless of the processing parameters. So, it is revealed from the present study that the usage of different ball sizes (3, 5 and 10 mm) during the mechanical milling has no influence on microstructure, mechanical and thermoelectric properties.

4. Conclusion

In summary, *p*-type $Bi_{0.5}Sb_{1.5}Te_3$ fine powders were successfully fabricated by MA and subsequently consolidated with an SPS technique. The milled powders and bulk samples exhibit single phase of $Bi_{0.5}Sb_{1.5}Te_3$ with rhombohedral structure. The relative density is obtained about 100% for the SPS-ed bulks. The average micro Vickers hardness is measured about ~100 Hv for all samples regardless of processing parameters. The low sintering temperature technique (SPS) gives very fine grain structure (1-4 μm sizes) in the matrix. The temperature dependence of TE properties was investigated, and the result revealed that the effect of the different ball sizes used in the MA process is negligible in ternary *p*-type $Bi_{0.5}Sb_{1.5}Te_3$ alloys.

Acknowledgements

This work was supported by 'Energy Efficiency & Resources Core Technology Program' of the Korea Institute of Energy Technology Evaluation and Planning (KETEP) granted financial resource from the Ministry of Trade, Industry & Energy, Republic of Korea (20152020001210).

References

[1] G. J. Snyder and E. S. Toberer: Nat. Mater., **7** (2008) 105.
[2] M. S. Dresselhaus, G. Chen, M. Y. Tang, R. G. Yang, H. Lee, D. Z. Wang, Z. F. Ren, J.-P. Fleurial and P. Gogna:

Adv. Mater., **19** (2007) 1043.
[3] L.E. Bell: Science, **321** (2008) 1457.
[4] T. C. Harman, P. J. Taylor, M. P. Walsh and B. E. LaForge: Science, **297** (2002) 2229.
[5] B. Poudel, Q. Hao, Y. Ma, Y. Lan, A. Minnich, B. Yu, X. Yan, D. Wang, A. Muto, D. Vashaee, X. Chen, J. Liu, M. S. Dresselhaus, G. Chen and Z. Ren: Science, **320** (2008) 634.
[6] C. H. Lim, D. C. Cho, Y. S. Lee and C. H. Lee: J. Korean Phys. Soc., **46** (2005) 995.
[7] R. Venkatasubramanian, E. Siivola, T. Colpitts and B. O'Quinn: Nature, **413** (2001) 597.
[8] B. Madavali, H.-S. Kim and S.-J. Hong: J. Electron. Mater., **43** (2014) 2390.
[9] H.-S. Kim and S.-J. Hong: J. Alloys Compd., **586** (2014) S428.
[10] T. Zhang, Q. S. Zhang, J. Jiang, Z. Xiong, J. M. Chen, Y. L. Zhang, W. Li and G. J. Xu: Appl. Phys. Lett., **98** (2011) 022104.
[11] Y. Ma, Q. Hao, B. Poudel, Y. Lan, B. Yu, D. Wang, G. Chen and Z. Ren: Nano Lett., **8** (2008) 2580.
[12] S. Jimenez, J. G. Pereza, T. M. Tritt, S. Zhub, J. L. S. Sancheza, J.-M. Juareza and O. López: Energy Convers. Manage., **87** (2014) 868.
[13] Z.-Y. Li, M. Zou and J.-F. Li: J. Alloys Compd., **549** (2013) 319.
[14] H. Li, H. Jing, Y. Han, G.-Q. Lu and L. Xu: Intermetallics, **43** (2013) 16.
[15] M. H. Bhuiyan, T.-S. Kim, J. M. Koo and S.-J. Hong: J. Alloys Compd., **509** (2011) 1722.
[16] X. A. Fan, J. Y. Yang, R. G. Chen, W. Zhu and S. Q. Bao: Mater. Sci. Eng. A, **438** (2006) 190.